Am. J. Hum. Genet. 70:435–447, 2002

Gdnf Haploinsufficiency Causes Hirschsprung-Like Intestinal Obstruction and Early-Onset Lethality in Mice

Liya Shen,[1,*] José G. Pichel,[2] Thomas Mayeli,[1] Hannu Sariola,[3] Bai Lu,[1] and Heiner Westphal[1]

[1]National Institute of Child Health and Human Development, National Institutes of Health, Bethesda; [2]Unidad de Investigación, Hospital de Mérida, Mérida, Spain; and [3]Institute of Biotechnology, University of Helsinki, Helsinki

Hirschsprung disease (HSCR) is a common congenital disorder that results in intestinal obstruction and lethality, as a result of defective innervation of the gastrointestinal (GI) tract. Despite its congenital origin, the molecular etiology of HSCR remains elusive for >70% of patients. Although mutations in the c-*RET* receptor gene are frequently detected in patients with HSCR, mutations in the gene encoding its ligand (glial cell line–derived neurotrophic factor [GDNF]), are rarely found. In an effort to establish a possible link between human HSCR and mutations affecting the *Gdnf* locus, we studied a large population of mice heterozygous for a *Gdnf* null mutation. This $Gdnf^{+/-}$ mutant cohort recapitulates complex features characteristic of HSCR, including dominant inheritance, incomplete penetrance, and variable severity of symptoms. The lack of one functioning *Gdnf* allele causes a spectrum of defects in gastrointestinal motility and predisposes the mutant mice to HSCR-like phenotypes. As many as one in five $Gdnf^{+/-}$ mutant mice die shortly after birth. Using a transgenic marking strategy, we identified hypoganglionosis of the gastrointestinal tract as a developmental defect that renders the mutant mice susceptible to clinical symptoms of HSCR. Our findings offer a plausible way to link an array of seemingly disparate features characteristic of a complex disease to a much more narrowly defined genetic cause. These findings may have general implications for the genetic analysis of cause and effect in complex human diseases.

Introduction

Hirschsprung disease (HSCR [MIM 142623]) is a common pediatric disorder, with an incidence of 1/5,000 live births (Ehrenpreis 1970; Holschneider 1982). The clinical symptoms are vomiting, abdominal distension, severe constipation, and intestinal obstruction, usually manifested shortly after birth. The main diagnostic criterion is the congenital absence of intrinsic ganglionic cells (aganglionosis) along the gastrointestinal (GI) tract. A typical "short segment" aganglionosis, together with a marked intestinal dilation (megacolon), is observed in the most distal regions of the GI tract. Sometimes, a more proximal "long segment" of the GI tract is affected as well. Severe intestinal-motility defects, resulting from regional aganglionosis, are incompatible with life and require surgical removal of the aganglionic segment. Occasionally, intestinal sections from patients with HSCR-like symptoms merely show a reduced number of ganglionic cells, a condition called hypoganglionosis. However, the pathogenesis of hypoganglionosis and its relationship to HSCR have not been established (Weinberg 1975; Holschneider 1982; Holschneider et al. 1994; Qualman and Murray 1994). Most patients with HSCR are infants born to healthy parents, and, in such cases, the disease appears to be sporadic. Approximately 20% of HSCR cases are familial, defined as more than one child in the same family affected by the disease. In familial HSCR, siblings of children with long and short segment HSCR are expected to develop the disease at a risk of 8.2%–19.1% and 2.6%–7.6%, respectively; both risk levels are several hundredfold higher than that of the general population (0.02%) (Badner et al. 1990).

So far, two signaling pathways have been linked to HSCR: endothelin 3 (EDN3 [MIM 131242]), with its receptor endothelin receptor type B (EDNRB [MIM 121244]), and GDNF, with its receptor c-RET ([MIM 164761]; for review, see Kapur 1999). The mutations in the *END3* and *EDNRB* loci, which account for most instances of the rare Shah-Waardenburg syndrome (WS4 [MIM 277580]), are present in <5% of patients with HSCR (Gershon 1995; Chakravarti 1996). By contrast, mutations in *c-RET* have been observed in as many as 25% of all patients with HSCR (Edery et al. 1994; Romeo et al. 1994; Yin et al. 1994; Angrist et

Received September 12, 2001; accepted for publication November 15, 2001; electronically published January 3, 2002.

Address for correspondence and reprints: Dr. Heiner Westphal, Laboratory of Molecular Genetics and Development, National Institute of Child Health and Human Development, National Institutes of Health, Building 6B, Room 413, Bethesda, MD 20814-2790. E-mail: hw@helix.nih.gov

* Present affiliation: Laboratory of Cellular Carcinogenesis and Tumor Promotion, National Cancer Institute, National Institutes of Health, Bethesda.

0002-9297/2002/7002-0016$15.00

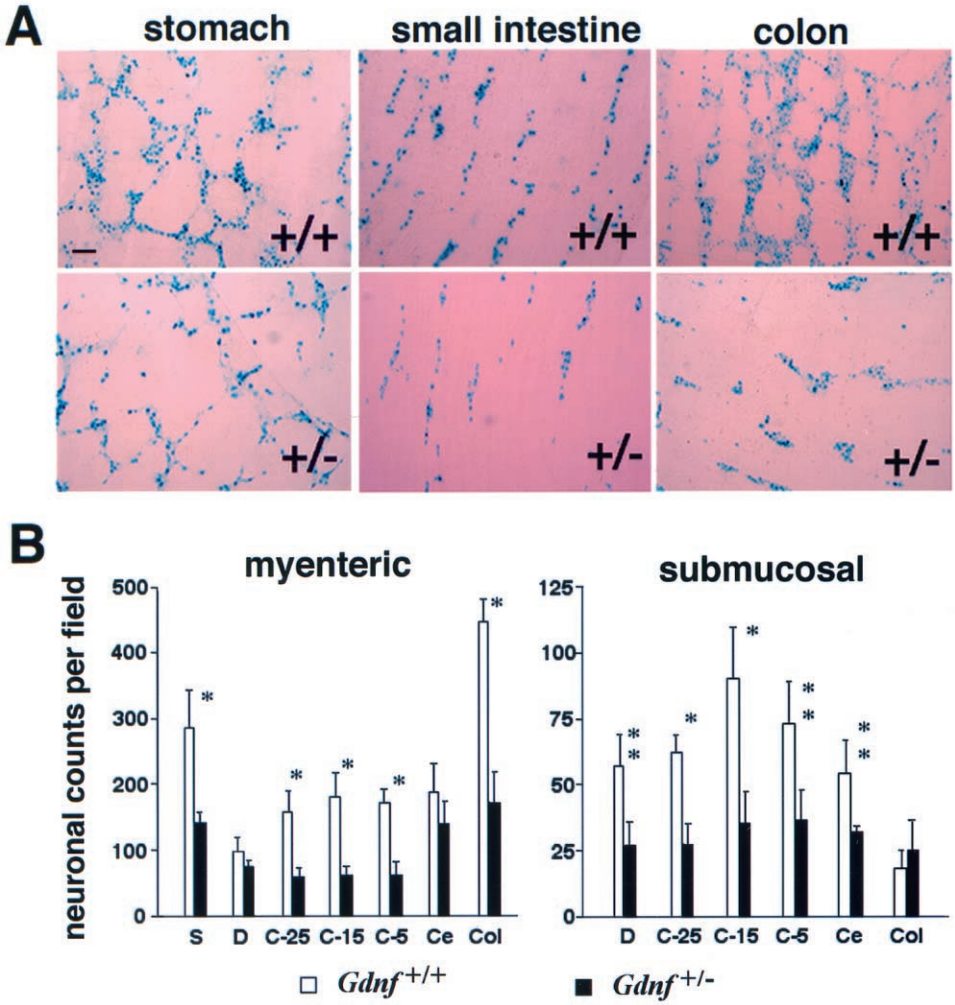

Figure 1 Quantitative analysis of neuronal densities along the GI tracts in adult $Gdnf^{+/+}$ and $Gdnf^{+/-}$ mice. $Gdnf^{+/-}$ mice were crossed with *DβH-nLacZ* transgenic mice, to mark enteric neurons in the GI tracts. *A*, X-gal staining of adult myenteric plexus formations in stomach, small intestine, and colon. After whole-mount staining, the X-gal–stained outer muscular layer and myenteric plexus were peeled from the rest of the intestinal wall and were mounted separately on glass slides. Bar = 100 μm. *B*, Neuronal counts per field of myenteric (*left*) and submucosal (*right*) plexi along the GI tracts of adult $Gdnf^{+/+}$ and $Gdnf^{+/-}$ mice. Average ganglionic cell counts per microscopic field in seven designated intestinal regions were obtained by counting LacZ-expressing cells at 4 × magnification. Four fields were counted in each region of the GI tract. S = stomach; D = duodenum; C-25 = 25 cm proximal to the cecum (jejunum); C-15 = 15 cm proximal to the cecum (proximal ileum); C-5 = 5 cm proximal to the cecum (distal ileum); Ce = cecum; Col = colon. Open bar, $Gdnf^{+/+}$, $N = 6$ animals; filled bar, $Gdnf^{+/-}$, $N = 6$ animals. Data in this and all other figures are presented as mean ± SEM. * = $P < .005$ and ** = $P < .02$, by Student *t* test.

al. 1995; Attié et al. 1995). The remaining >70% of patients with HSCR have not been linked to specific genetic defects, posing great challenges to our understanding of the disease etiology (Puri et al. 1998). Very few HSCR cases have been associated with mutations in the gene encoding GDNF, the ligand for c-RET (Angrist et al. 1996; Ivanchuk et al. 1996; Salomon et al. 1996). Biochemical studies have shown that the GDNF level is reduced in aganglionic segments of the GI tract (Bär et al. 1997; Martucciello et al. 1998; Ohshiro and Puri 1998). However, there is no direct genetic evidence to implicate *GDNF* as a major susceptibility locus for human HSCR.

Some animal models have provided insights into the mechanism of HSCR pathogenesis. Patterns of autosomal recessive HSCR are reflected by targeted or spontaneous mutations of the EDN3/EDNRB pathway in mice (Baynash et al. 1994; Hosoda et al. 1994; Puffenberger et al. 1994; Edery et al. 1996). These mutant strains mimic the Shah-Waardenburg syndrome, with respect to the occurrence of megacolon and distal colon aganglionosis, the juvenile age at onset, the recessive

inheritance, the high penetrance of symptoms, and the presence of associated defects that include depigmentation and deafness (Kusafuka and Puri 1997; Kapur 1999). Mice that lack the function of *c-Ret* are devoid of ganglionic cells in the entire GI tract and lack both kidneys (Schuchardt et al. 1994). Similar phenotypes are seen in mice with mutations in other components of the c-Ret pathway, *Gdnf* and *Gfrα1* (Moore et al. 1996; Pichel et al. 1996; Sánchez et al. 1996; Cacalano et al. 1998; Enomoto et al. 1998). The studies cited in the preceding sentence have shown that GDNF/c-RET signaling pathway is crucial for enteric nervous system development and kidney organogenesis, but none of the null mutant mice display genetic features characteristic of human HSCR. Appropriate animal models for the common, nonsyndromic HSCR do not yet exist; however, when they are established, they will improve our understanding of disease pathogenesis for the dominant HSCR.

Elsewhere, we have reported a spectrum of abnormal kidney morphology in a subset of mice that lack one functioning *Gdnf* allele (Pichel et al. 1996). We report here that this mutant cohort is also characterized by incomplete penetrance and variable expressivity of Hirschsprung-like intestinal obstruction. As many as one of every five $Gdnf^{+/-}$ mice dies before weaning. Our study, which involves large cohorts of *Gdnf* mutant mice in three different genetic backgrounds, implicates *GDNF* as a major HSCR susceptibility locus in humans.

Material and Methods

Animals and Genotyping

Gdnf-null mutant mice were generated as described elsewhere (Pichel et al. 1996). The mutant mice were maintained by two to five generations of backcrossing either into inbred C57BL/6 or 129/Sv strains or into the outbred CD1 strain. $Gdnf^{+/-}$ progeny of these crosses were mated with $D\beta H\text{-}nLacZ^{+/+}$ mice to obtain $Gdnf^{+/-}$, $D\beta H\text{-}nLacZ^{+/-}$ animals. Primers used for PCR genotyping were as follows: *Gdnf* knockout allele (255 bp; 5′-CGGAGCCGGTTGGCGCTACCGG-3′ and 5′-ACGACTCGGACCGCCATCGGTG-3′); *Gdnf* wild-type allele (337 bp; 5′-GAGAGGAATCGGCAGGCTG-CAGCTG-3′ and 5′-CAGATACATCCACATCGTTTA-GCGG-3′); and LacZ primer set (278 bp; 5′-ACCCAAC-TTAATCGCCTTGC-3′ and 5′-AACAAACGGCGGAT-TGACC-3′.

Quantitative Analysis of Enteric Neuronal Density

Embryonic or adult GI tracts were fixed in 4% paraformaldehyde at 4°C for 0.5–2 h in 0.1M $NaPO_4$ buffer (pH 7.2) and were washed extensively in X-gal staining buffer. Whole-mount X-gal staining was performed in the dark, with freshly prepared X-gal staining solution (Kapur et al. 1991; Mercer et al. 1991). To obtain accurate neuronal counts in a region-specific manner, we dissected small segments at defined locations along the GI tract of adult mice and were mounted the myenteric and submucosal plexi separately on glass slides. This was achieved by separating the outer muscular layers, which contain the myenteric plexus, from the submucosal plexus and mucosa after X-gal staining. The intestinal tissues were not stretched during the fixing, staining, or mounting processes. Duodenum was dissected from regions caudal to the pyloric junction. Regions of small intestine were defined on the basis of their relative distance (in centimeters) from the cecum. The colon specimens were taken from a region of colon that was 4 cm distal of the cecum. For an accurate quantification of neuronal density (X-gal–positive nuclear staining) and for direct comparison of ganglionic cell densities in different regions, four images, under the same magnification, were captured per region in each GI tract, using a CG7-frame grabber with Nikon Microphot microscopy (Scion). The neuronal density was quantified with an National Institutes of Health image program.

Genetic Analysis of Mortality in the Preweaning Period

Mortality in the preweaning period was calculated on the basis of the difference between the number of expected and the number of observed $Gdnf^{+/-}$ offspring, as determined by genotyping at weaning. Before birth, Mendelian segregation of *Gdnf* alleles was well preserved (24.2% $Gdnf^{+/+}$, 51% $Gdnf^{+/-}$, and 24.8% $Gdnf^{-/-}$; $N = 557$). If we assume equal likelihood of accidental death in the preweaning period for pups of both the $Gdnf^{+/+}$ and the $Gdnf^{+/-}$ genotypes, the number of $Gdnf^{+/-}$ weanlings derived from a $Gdnf^{+/+} \times Gdnf^{+/-}$ cross was expected to be the same as that of $Gdnf^{+/+}$ weanlings. As mentioned before, $Gdnf^{-/-}$ mice die at birth. Thus, two-thirds of weanlings derived from a $Gdnf^{+/-}$ by $Gdnf^{+/-}$ cross were expected to be $Gdnf^{+/-}$, the remaining one-third being wild-type littermates. The statistical significance of the increased preweaning mortality of $Gdnf^{+/-}$ mice was determined by χ^2 analysis.

Results

Significantly Reduced Enteric Innervation in Adult and Embryonic $Gdnf^{+/-}$ GI Tracts

We used a quantitative transgenic marking strategy to assess the number and mesh density of enteric neurons and to discern subtle differences in the number of enteric neurons between $Gdnf^{+/+}$ and $Gdnf^{+/-}$ GI tracts. $Gdnf^{+/-}$ mice were crossed with the $D\beta H\text{-}nLacZ$ transgenic strain, in which the nuclei of enteric gangli-

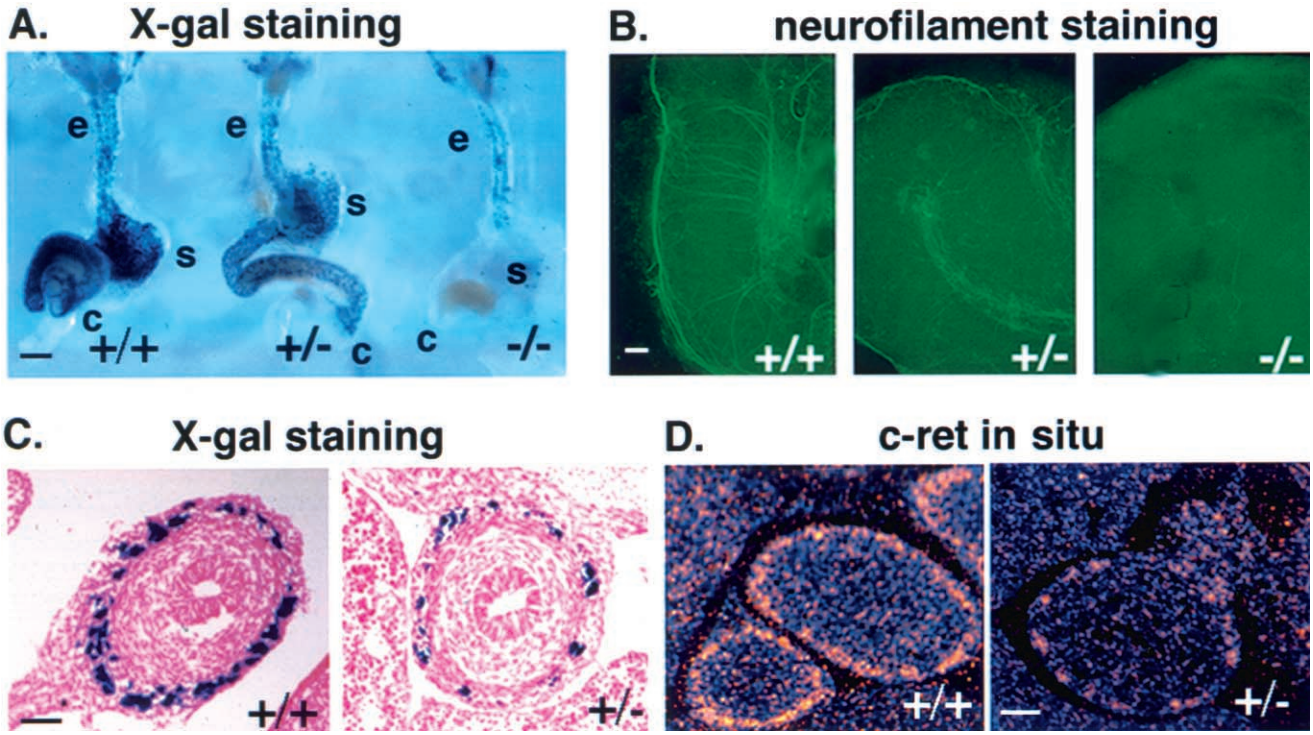

Figure 2 *Gdnf* gene dosage dependence of enteric innervation in developing mouse embryos. *A,* Whole-mount X-gal staining of GI tracts of E11.5 $Gdnf^{+/+}$, $Gdnf^{+/-}$, and $Gdnf^{-/-}$ embryos derived from F2 progeny of $Gdnf^{+/-}$ × *DβH-nLacZ* crosses. e = esophagus; s = stomach; c = cecum. The blue spots represent individual nuclei of enteric neuronal precursor cells. Note the significant reduction in the number of LacZ-expressing cells in $Gdnf^{+/-}$ and their absence in $Gdnf^{-/-}$ stomach (s) and cecum (c), but not in esophagus (e). Bars = 200 μm. *B,* Whole-mount immunostaining of E11.5 mid–GI tract explants using anti-neurofilament antibody. Neuronal precursor cells and their processes were visualized in mid–GI tract explants cultured for 72 h, using a fluorescein-conjugated secondary antibody. Bar = 100 μm. *C,* Transverse sections of X-gal–stained GI tracts of E12.5 embryos derived from F2 progeny of a $Gdnf^{+/-}$ × *DβH-nLacZ*$^{+/+}$ cross. The number of *LacZ*-expressing cells is greatly reduced in the $Gdnf^{+/-}$ section. Bar = 50 μm. *D, c-Ret* in-situ hybridization of transverse sections of E14.5 $Gdnf^{+/+}$ and $Gdnf^{+/-}$ intestines. The *c-Ret* mRNA signal is markedly reduced in cells of the myenteric layer of the $Gdnf^{+/-}$ section. Bar = 50 μm.

onic cells express the bacterial β-galactosidase reporter gene under the control of a human dopamine β-hydroxylase gene promoter (Kapur et al. 1991; Mercer et al. 1991). Whole-mount staining of GI tracts provided a sensitive and quantitative measurement of the density of the X-gal–targeted enteric ganglionic cells, thereby allowing unambiguous region-by-region comparison of GI tracts at various ages. Figure 1*A* shows representative X-gal staining of myenteric plexus formations of stomach, small intestine, and colon. Quantitative analysis indicated that the numbers, as well as the mesh density, of ganglionic cells were clearly reduced in both the myenteric and the submucosal plexus formations in adult $Gdnf^{+/-}$ GI tracts (fig. 1*A* and *B*). In the $Gdnf^{+/-}$ GI tracts, cell numbers were reduced by 64% ($P < .002$) in the ileocecum and colon and by 50% in stomach ($P < .05$) and small intestine ($P < .04$). Moreover, the weblike connections of myenteric plexi, as well as the cell density in individual myenteric plexus formations, were severely diminished in adult $Gdnf^{+/-}$ colons (fig. 1*A*). Thus, there is a general hypoganglionosis in $Gdnf^{+/-}$ GI tracts, and the terminal intestine may be more sensitive to a reduction in *Gdnf* gene dosage.

To define the developmental origin of hypoganglionosis of $Gdnf^{+/-}$ animals, we performed X-gal staining of embryonic GI tracts. *Gdnf* gene dosage-dependent differences in the number of X-gal–positive cells were detected as early as embryonic day (E) 10, as soon as the migrating enteric precursor cells arrive in the developing stomach (data not shown). At E11.5, extensive X-gal–positive cells reached the ileocecal junction in $Gdnf^{+/+}$ embryos (fig. 2*A*). Consistent with previous findings that enteric neuronal precursors of both vagal and sacral crest origins are defective in the absence of GDNF (Durbec et al. 1996; Pichel et al. 1996), few, if any, X-gal–positive cells were present beyond the esophagus in the $Gdnf^{-/-}$ intestine (fig. 2*A*). Significantly, X-gal staining revealed a reduction in the density of the enteric precursors in $Gdnf^{+/-}$ mutants (fig. 2*A* and *C*). As a consequence, fewer neuronal processes, as revealed by whole-mount antineurofilament immunostaining, were present in $Gdnf^{+/-}$ intestines as compared with

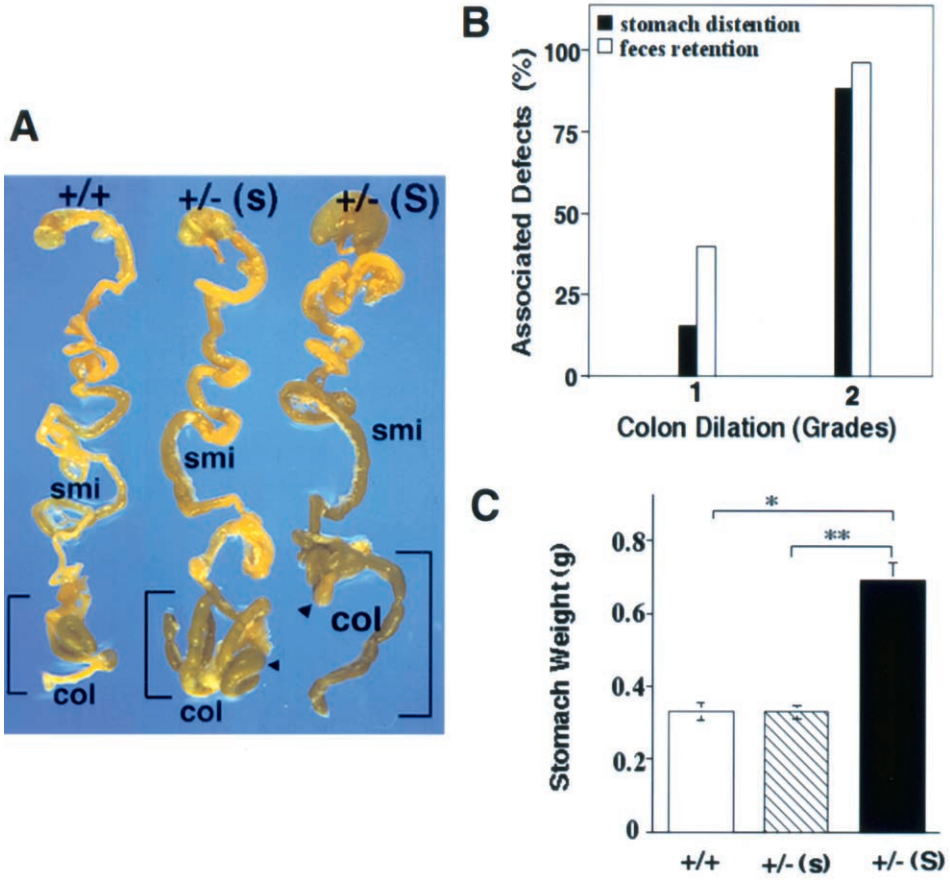

Figure 3 Spectrum of intestinal-motility defects in adult $Gdnf^{+/-}$ mice. *A*, Examples of intestinal-motility defects. GI tracts dissected from a $Gdnf^{+/+}$ mouse, a $Gdnf^{+/-}$ mouse with fecal retention but normal stomach ($Gdnf^{+/-}$[s]), and a $Gdnf^{+/-}$ mouse with severe fecal retention and stomach distention [$Gdnf^{+/-}$(S)]. smi = small intestine; col = colon. *B*, Association of colon dilation with other deficits in the $Gdnf^{+/-}$ cohort. The severity of the colon dilation is defined qualitatively: Grade 1 = small to mild dilation, 1.3–2.0 × the width of the $Gdnf^{+/+}$ colon; Grade 2 = severe colon dilation, >2 × the $Gdnf^{+/+}$ colon width. Stomach distention is defined as >1.5 × the normal $Gdnf^{+/+}$ stomach size after 2–6 h of fasting (as marked by "S" in panel *A*). Fecal retention is defined as (1) a greatly increased number of fecal pellets, in comparison with the number seen in the $Gdnf^{+/+}$ control or (2) a continuous string of pellets along the length of the large intestine. The percentage of animals with stomach distention or fecal retention was calculated for animals with grade 1 or 2 colon dilation, respectively, and was also noted in a small fraction (<5%) of control mice. *C*, Average weight of stomachs derived from $Gdnf^{+/+}$ ($N = 28$), $Gdnf^{+/-}(s)$ ($N = 27$), and $Gdnf^{+/-}(S)$ ($N = 30$) mice. * = $P < .0001$ (Student *t* test).

those in $Gdnf^{+/+}$ controls (fig. 2*B*). In parallel, there was a reduced density of c-Ret expressing cells, as visualized by in situ hybridization (fig. 2*D*). Taken together, these results underscore the quantitative effect of Gdnf signaling on the development of c-Ret–expressing enteric precursors and suggest an anatomical and pathogenetic basis for HSCR susceptibility in $Gdnf^{+/-}$ mice.

Significantly Compromised Intestinal Motility in Adult and Newborn Gdnf$^{+/-}$ *Mice*

To determine whether hypoganglionosis causes functional impairment in adult $Gdnf^{+/-}$ mice, we examined 172 adult animals (37 $Gdnf^{+/+}$ and 135 $Gdnf^{+/-}$) for possible defects in intestinal motility. The $Gdnf^{+/-}$ GI specimens revealed varying degrees of colon dilation (84%), fecal retention (74%), and stomach distention (38.5%). In contrast, <5% of the GI tracts dissected from $Gdnf^{+/+}$ animals showed stomach distention or fecal retention. The high percentage of mice with fecal retention, a sign of chronic constipation, correlates well with greater reduction of neuronal counts at the terminal intestine. The normal GI tract (fig. 3*A*) shows discretely segregated fecal pellets that result from a propulsive intestinal movement controlled by intrinsic enteric neuronal circuits (Gershon et al. 1994; Milla 1996). The efficiency of movement was apparently impaired in $Gdnf^{+/-}$ mutants, because fecal retention, especially in the colon, was very common (fig. 3*A*). Stomach distention was less common and was often accompanied by

more-severe fecal retention and a backup of processed food into a substantial portion of the small intestine (fig. 3*A*). We graded the degree of colon dilation semiquantitatively, assigning values as follows: grade 0 indicates no dilation, $Gdnf^{+/+}$ colon width; grade 1 indicates small-to-moderate dilation, 1.3–2 times as great as that of $Gdnf^{+/+}$ colon width; and grade 2 indicates severe colon dilation, i.e., >2 times that of $Gdnf^{+/+}$ colon width. In $Gdnf^{+/-}$ mice, an increase in stomach size was often associated with grade 2 intestinal dilation (fig. 3*B* and *C*). Taken together, our observations strongly suggest a causal relationship between a loss of a functional *Gdnf* allele and the presence of hypoganglionosis and widespread intestinal dysmotility in the adult $Gdnf^{+/-}$ cohorts.

To evaluate a possible clinical manifestation of impaired intestinal innervation in younger $Gdnf^{+/-}$ mice, we noninvasively assessed functional consequences of hypoganglionosis in newborn mice. We recorded the time interval between last feeding and the disappearance of the "milk spot" (i.e., milk-filled stomach readily visible through the skin of the neonate). This time interval was 20 ± 4 h in $Gdnf^{+/-}$ mutants ($N = 8$), and 5 ± 1 h in $Gdnf^{+/+}$ littermates ($N = 5$). The delayed gastric emptying in newborn $Gdnf^{+/-}$ mutants suggests that enteric hypoganglionosis causes impaired intestinal motility at birth, consistent with the developmental origin of hypoganglionosis. The varying severity of intestinal dysmotility points to a clinical predisposition to HSCR-like symptoms in the $Gdnf^{+/-}$ cohort.

Severe Hypoganglionosis and/or Segmental Aganglionosis in Gdnf$^{+/-}$ *Mice*

Human HSCR is based on segmental aganglionosis that is typically observed in the distal colon (Ehrenpreis 1970; Holschneider 1982). To determine whether an HSCR-like pathology could exist in the $Gdnf^{+/-}$ cohort, we focused on the density of ganglionic cells in the GI tracts of the mutant mice. In our experiments, we defined aganglionosis as an absence of—and hypoganglionosis as a reduction in—the number of X-gal staining cells. We examined a large number of mice—at various stages of life, from neonatal to adulthood—for variations in enteric innervation. In adult $Gdnf^{+/-}$ GI tracts, we not only found a general reduction in the number of X-gal–positive cells, but we also frequently observed intestinal segments, of variable length, that were entirely devoid of them (see the example shown in fig. 4*A*). These seemingly aganglionic regions were interspersed along the hypoganglionic regions of the intestine (fig. 1*A*). Aganglionosis was never observed in $Gdnf^{+/+}$ GI tracts. However, figure 4*A* shows a rare example of hypoganglionosis in a $Gdnf^{+/+}$ intestine. Regional variation of neural density occurs in both $Gdnf^{+/+}$ and $Gdnf^{+/-}$ GI tracts. Such a variation may explain why we saw regions almost devoid of X-gal staining in predominantly hypoganglionic $Gdnf^{+/-}$ mice (fig. 4*C*) and occasional hypoganglionosis in normal animals (fig. 4*B*). Thus, regional aganglionosis, which is most commonly found in the small intestines, occurs in adult $Gdnf^{+/-}$ mice that do not have HSCR.

In human pathology, the diagnosis of HSCR is based on the absence of ganglionic cells (aganglionosis) from serial sections of intestinal biopsies. Hypoganglionosis in the context of HSCR is rarely documented by this procedure. To better relate our whole-mount X-gal staining results to those obtained by serial sections of human intestinal tissue, we examined transverse sections of $Gdnf^{+/-}$ mutant intestinal specimens. We found significantly more aganglionosis than hypoganglionosis in $Gdnf^{+/-}$ intestinal specimens. Fig. 4*D* shows an example of seemingly aganglionic or severely hypoganglionic pathology in a transverse $Gdnf^{+/-}$ colon section, compared with a wild-type control. The very few enteric neurons in the $Gdnf^{+/-}$ colon section shown here could be easily missed were they not marked by X-gal staining. The peeled myenteric spreads (figs. 4*B* and 4*C*) that we used as a basis for the assessment of ganglionic density are ~1 mm, which is equivalent to 2% of the length of an adult mouse colon. This amounts to ~200 consecutive 5-μm intestinal sections, as shown in figure 4*D*. It follows that a distinction between severe hypoganglionosis and aganglionosis, based on the examination of a limited number of cross sections of intestinal tissue, is difficult to make. Thus, hypoganglionosis in the context of a variety of intestinal dysmotility and HSCR may be much more widespread than has hitherto been recognized.

Low Penetrance of Early-Onset Lethality in the Gdnf$^{+/-}$ *Cohort*

Severe hypoganglionosis and aganglionosis were also observed in some of the X-gal-stained newborn $Gdnf^{+/-}$ intestinal specimens. Figure 5*C* shows an example of a peeled myenteric plexus from a newborn $Gdnf^{+/-}$ mouse in which approximately half of the entire GI tract was aganglionic and the rest severely hypoganglionic, compared to whole-mount X-gal staining of GI tracts from $Gdnf^{+/+}$ and $Gdnf^{+/-}$ controls shown in figures 5*A* and 5*B*. Mice with such severe aganglionosis are unlikely to survive. In human HSCR, segmental aganglionosis causes intestinal obstruction, and, if untreated, most patients with HSCR die within the first year of life. Treatments include temporary relief of obstruction by repeated enema and, ultimately, by surgical removal of aganglionic GI segments. High mortality (67%) is associated with long-segment HSCR, regardless of treatment (Badner et al. 1990; Berry and Keeling 1996). In an effort to determine whether a severe reduction

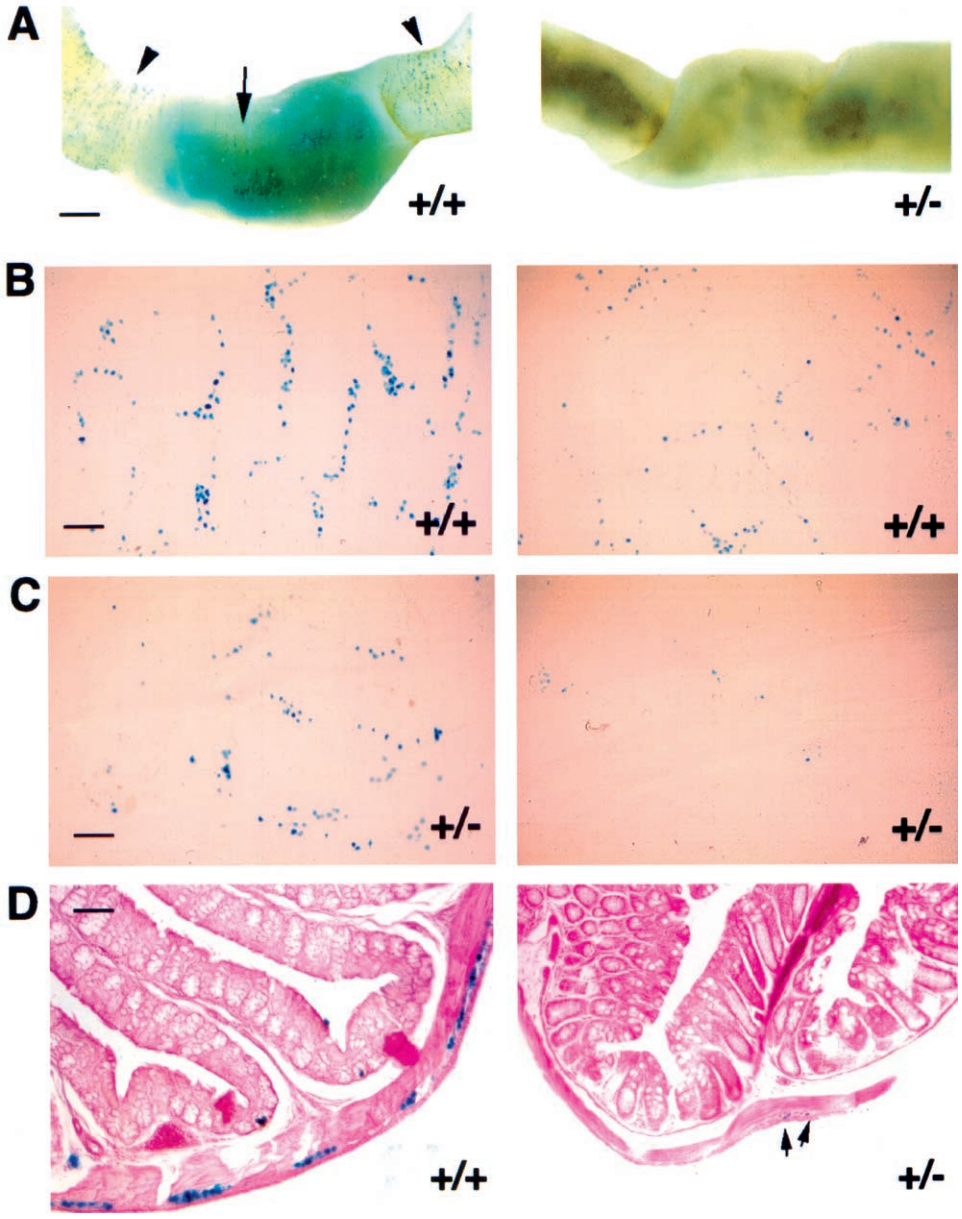

Figure 4 Enteric hypoganglionosis and aganglionosis in adult $Gdnf^{+/-}$ mice revealed by X-gal staining in whole-mount preparations and on sections. *A*, Regional variation of X-gal–stained ganglionic cell density in adult $Gdnf^{+/+}$ and $Gdnf^{+/-}$ GI tracts. *Left*, an occasional and limited hypoganglionic segment in a $Gdnf^{+/+}$ intestine (*arrow*) flanked by normal ganglionosis (arrowhead). Bar = 1 mm. *Right*, a portion of segmental aganglionosis in $Gdnf^{+/-}$ small intestine. *B*, Normal and hypoganglionic myenteric plexus of the small intestine from an adult $Gdnf^{+/+}$ mouse. Bar = 100 μm. *C*, Hypoganglionic and almost aganglionic myenteric plexus of the small intestine from an adult $Gdnf^{+/-}$ mouse. Bar = 100 μm. *D*, X-gal–stained transverse sections through a P17 $Gdnf^{+/+}$ colon (normal ganglionic) and a P17 $Gdnf^{+/-}$ colon (aganglionic). *Arrowheads* indicate X-gal positive ganglionic cells. Bar = 20 μm.

in enteric ganglion density can result in early-onset lethality in our mutant mice as well, we examined whether there is a preferential loss of $Gdnf^{+/-}$ mice prior to weaning. Up to the date of birth, Mendelian segregation of *Gdnf* alleles was well preserved (24.2% $Gdnf^{+/+}$, 51% $Gdnf^{+/-}$, and 24.8% $Gdnf^{-/-}$ [N = 557]). As reported above, nearly all animals that died within the first 24 h were homozygous *Gdnf*-null mutants (Moore et al. 1996; Pichel et al. 1996; Sánchez et al. 1996). Nearly all pups that died after the first 24 h were $Gdnf^{+/-}$. Neither $Gdnf^{-/-}$ nor $Gdnf^{+/-}$ pups that were found dead exhibited gross signs of GI dilation. The extent of $Gdnf^{+/-}$ lethality in the preweaning period was calculated on the basis of the

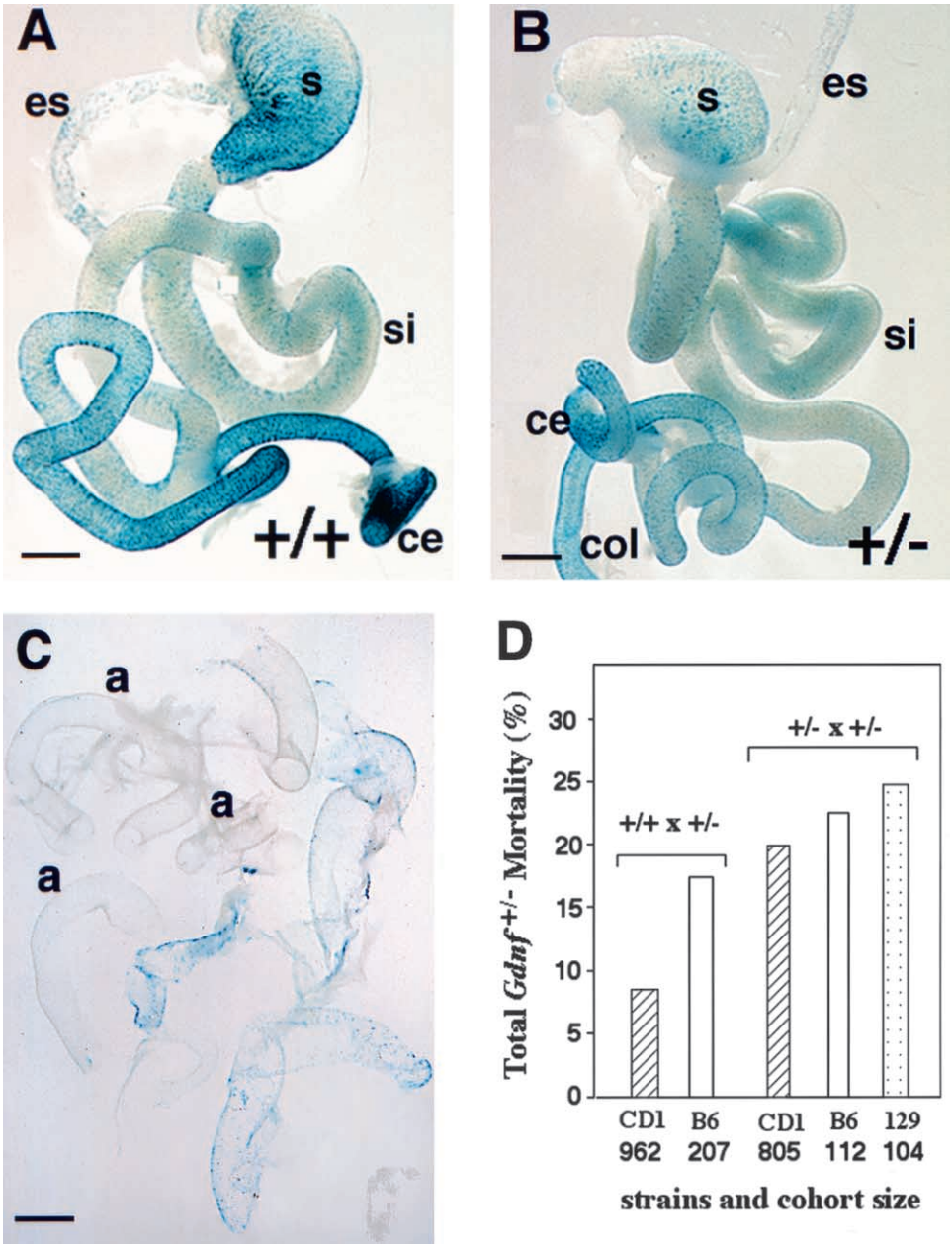

Figure 5 Preweaning lethality in $Gdnf^{+/-}$ population by pathological and genotyping analysis *A*, Overview of myenteric plexus from a $Gdnf^{+/+}$ newborn mouse. Bar = 1 mm. *B*, Overview of myenteric plexus from a $Gdnf^{+/-}$ newborn mouse. es = esophagus; si = small intestine; ce = cecum; and col = colon. Bar = 1 mm. *C*, Example of extensive aganglionosis and severe hypoganglionosis in a newborn $Gdnf^{+/-}$ mouse. Shown here are the pieces of myenteric plexus peeled from the GI tract of a single newborn $Gdnf^{+/-}$ mouse after whole-mount X-gal staining; a = aganglionosis. Bar = 1 mm. *D*, Preweaning lethality in $Gdnf^{+/-}$ population. Preweaning mortality = [the number of expected $Gdnf^{+/-}$ mice − the number of observed $Gdnf^{+/-}$ offspring at weaning]/total number of expected births (on the basis of genotyping at weaning). The expected number of $Gdnf^{+/-}$ mice is equal to $Gdnf^{+/+}$ in $Gdnf^{+/+}$ × $Gdnf^{+/-}$ crosses (twice the wild-type number in $Gdnf^{+/-}$ × $Gdnf^{+/-}$ crosses). Mating schemes and names of strains used in the crosses are listed in the figure. CD1 is an outbred strain, and B6 (C57BL/6) and 129 (129/Sv) are two inbred strains.

numerical difference between observed and expected $Gdnf^{+/-}$ genotypes at weaning. Our results show that a low, but highly significant, preweaning lethality is associated with *Gdnf* heterozygosity (fig. 5*D*).

We determined the influence of genetic background on the penetrance of the lethal phenotype using two different mating schemes. The preweaning lethality was 8.4% when the mutant *Gdnf* allele was maintained in

an outbred CD1 strain ($Gdnf^{+/-} \times Gdnf^{+/+}$; $N = 962$, $P < .01$) (fig. 5*D*), and it increased to 17.1% when the mutant *Gdnf* allele was backcrossed to the inbred C57BL/6 strain ($Gdnf^{+/-} \times Gdnf^{+/+}$; $N = 207$, $P < .001$; fig. 5*D*). Moreover, interbreeding of $Gdnf^{+/-}$ offspring from the outbred CD1 strain, but not from C57BL/6 or 129/Sv background, resulted in a significant increase (from 8.4% to 16.7%) in overall mortality for the CD1 strain ($P < .05$), and a loss of strain-dependent difference in mortality (16.7%–24.7%, $N = 805$, 112, 104, respectively; $P > .5$, fig. 5*D*). The sex ratio for the surviving 80%–90% $Gdnf^{+/-}$ mice remained at 1:1, suggesting a lack of sex bias on lethality in the $Gdnf^{+/-}$ cohort. We noted unilateral kidney agenesis in ~10% of our $Gdnf^{+/-}$ animals, confirming our earlier observation (Pichel et al. 1996). However, pathological examination failed to establish kidney dysfunction as the cause of death. Rather, our results support the notion that a subpopulation of the $Gdnf^{+/-}$ mice is predisposed to develop segmental aganglionosis and severe hypoganglionosis that are incompatible with life. Increased homozygosity at modifier loci may well influence the mortality rate.

Discussion

Our study of mice that are heterozygous for a null mutation in the GDNF gene has uncovered defects in enteric innervation and intestinal motility and a low, but highly significant, incidence of postnatal death. The phenotype of these mice reflects important aspects of Hirschsprung disease, in particular those seen in patients who carry mutations in components of the c-RET signaling pathway. There is a close resemblance among major parameters, including inheritance pattern, penetrance, expressivity, and age at onset of symptoms. The apparent phenotypic complexity revealed by our analysis of these mutant mice is based on *Gdnf* haploinsufficiency. Our results provide direct genetic evidence linking the *Gdnf* locus to HSCR etiology.

We assessed in different ways the possibility that a defined genetic defect affecting *Gdnf* gene dosage could elicit a broad spectrum of anatomical changes and disease symptoms that are typical of human HSCR. First, we examined the phenotypic consequences of a lack of one functioning *Gdnf* allele in several genetic backgrounds. The results suggested to us an involvement of second-site modifiers. Second, to study disease susceptibility, we used a population genetics approach, examining phenotypic variations in a large cohort of mutant mice. Third, in an effort to understand the apparent low penetrance and sporadic occurrence of HSCR in human patients, we employed an enteric ganglion–marking strategy to distinguish susceptible individuals from nonsusceptible ones in our mouse mutant cohorts and to diagnose the disease objectively. We took the following precautions to ensure that the difference in ganglionic cell density accurately reflects *Gdnf* gene function, rather than random fluctuation of X-gal staining. (1) The neuronal density and plexus pattern were independent of the copy number of the *LacZ* transgene (data not shown) but were dependent on *Gdnf* gene dosage. (2) $Gdnf^{+/+}$ and $Gdnf^{+/-}$ GI tracts were derived from the same litters and were stained at the same time. (3) The change in enteric density along the GI tract correlated well with the density of c-Ret–expressing cells. (4) The same staining of the X-gal–positive cells of $Gdnf^{+/-}$ intestinal specimens that exhibited regional aganglionosis also showed a general hypoganglionosis. In contrast, aganglionosis was never observed in $Gdnf^{+/+}$ control animals.

The low incidence and the variable severity of disease phenotypes are addressed in the model of figure 6. The model is based on the current state of knowledge with regard to neural crest innervation of the vertebrate GI tract (Burns and Le Douarin 1998, and references cited therein) and on our observations on $Gdnf^{-/-}$ and $Gdnf^{+/-}$ mutant mice. In the schematic drawing, we compare embryonic GI tract innervation in four scenarios: (1) $Gdnf^{+/+}$, (2) $Gdnf^{+/-}$ with an asymptomatic phenotype (defined here as non-lethal), (3) $Gdnf^{+/-}$ with a lethal phenotype, and (4) $Gdnf^{-/-}$. The presence of neuronal precursors derived from the neural crest is indicated by dots, the relative frequency of which depends on the genotype and the position along the GI tract. Vagal neural crest cells innervate the entire GI tract. Crest cells derived from the anterior trunk region colonize the esophagus and the proximal part of the stomach, and sacral neural crest cells contribute mostly to the innervation of the terminal intestine. Enteric ganglionic cells, which are missing in mice that are homozygous for mutations in components of the c-Ret signaling pathway, are derived from vagal and sacral neural crest precursor cells. By contrast, cells derived from the anterior trunk region are retained in those mutants (see the diagram labeled "$Gdnf^{-/-}$" in fig. 6). Precursor-cell density is highest in the distalmost part of the intestine, with dual contributions from both vagal and sacral crest, possibly reflecting special functional requirements in this area of the GI tract (Ehrenpreis 1970). It is precisely here that we see the greatest variability in the degree of hypoganglionosis in our $Gdnf^{+/-}$ mutant animals. While all $Gdnf^{+/-}$ animals are hypoganglionic when compared with the $Gdnf^{+/+}$ control, the observed spread in ganglionic cell counts of the distal GI tract correlated directly with the variable expressivity of intestinal dysmotility defects. A limited reduction in ganglionic cell density will be asymptomatic, as indicated in the diagram "$Gdnf^{+/-}(a)$" in figure 6. However, below a certain threshold level of distal intestinal innervation,

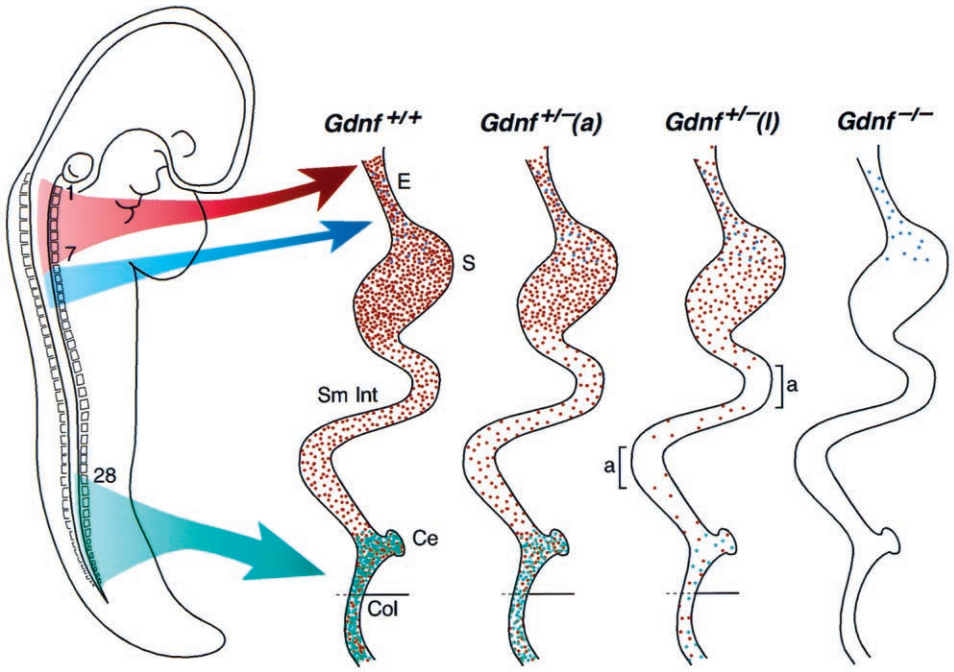

Figure 6 Schematic drawing of enteric innervation in normal and *Gdnf* mutant mice. This model addresses the incomplete penetrance and variable expressivity of symptoms resulting from *Gdnf* haploinsufficiency. The drawing on the left shows the migration paths of neural crest cells (enteric neuronal precursors) emanating from the dorsal midline at the time of neural-tube closure. Numbers indicate somite positions. Dots in the four drawings to the right are color coded according to the respective migration routes. They mark the position of neuronal precursors of late-gestation embryos along the GI tract. Vagal neural crest cells (*red,* somite 1–7) innervate the entire GI tract. Crest cells derived from the anterior trunk region (*blue*) colonize the esophagus and the proximal part of the stomach, and sacral crest cells (*green,* beyond somite 28) contribute to the innervation of the post-umbilical colon. The density and distribution of dots in the four drawings to the right reflects the neuronal counts obtained in normal and mutant mice. $Gdnf^{+/+}$ = $Gdnf^{+/+}$ control; $Gdnf^{+/-}(a)$ = asymptomatic $Gdnf^{+/-}$; $Gdnf^{+/-}(l)$ = lethal $Gdnf^{+/-}$; and $Gdnf^{-/-}$ = *Gdnf*-null mutants. Bracketed regions in $Gdnf^{+/-}(l)$ represent aganglionic segments, suggesting a further reduction of neuronal density from the level of asymptomatic $Gdnf^{+/-}(a)$ control. E = esophagus; S = stomach; Sm Int = small intestine; Ce = cecum; Col = colon.

lethal intestinal obstruction will ensue. Such a situation is depicted in the diagram "$Gdnf^{+/-}(l)$" in figure 6. We suggest that similar scenarios may play out in human HSCR, in which the degree of hypoganglionosis may well be a crucial determinant of the ensuing disease phenotype. Our results have shown that whole-mount staining techniques, presently not available in human pathology, are required to properly assess the levels of ganglionic cell density.

Burns and Le Douarin (1998) have discussed and referenced in detail findings in support of an interaction between vagal and sacral crest cells during colonization of the hindgut of both avian and mammalian embryos. Furthermore, their study of chick/quail chimeras directly demonstrates that sacral crest cells indeed contribute to terminal intestinal innervation. The present study, as well as findings published elsewhere (Schuchardt et al. 1994; Durbec et al. 1996; Moore et al. 1996; Pichel et al. 1996; Sánchez et al. 1996; Cacalano et al. 1998; Enomoto et al. 1998), indicate that a functional c-Ret signaling pathway is obligatory for GI tract innervation by both vagal and sacral crest derivatives, because all neuronal cells are missing from the intestine of *c-Ret*, *Gdnf*, and *Gfrα1* homozygous null mutants. In mice, no markers are presently available that would distinguish enteric neuronal precursors derived from the vagal crest from those of sacral crest origin. In $Gdnf^{+/-}$ mice, we see a disproportional loss and a high variability in the number of DβH-LacZ–positive cells in the distal-most part of the intestine, suggesting that the sacral crest derivatives are more likely to be affected by the loss of a functioning *Gdnf* allele than are cells derived from the vagal crest. On the basis of these considerations, our model in figure 6 postulates that the sacral crest contributes to post-umbilical intestinal innervation in the mammalian embryo as well. Migration of sacral crest–derived cells to the postumbilical intestine is independent of vagal crest cell migration, as demonstrated by previous lineage-tracing studies (Pomeranz and Gershon 1990; Pomeranz et al. 1991; Serbedzija et al. 1991). However, further development of sacral crest–derived enteric precursors into

Table 1

Genetic Features of Patients with HSCR and in *Gdnf*$^{+/-}$ Mice

Characteristic	Patients	Mice
Inheritance pattern	Dominant (c-RET mutations)	Dominant (*Gdnf*)
Penetrance	Incomplete	Incomplete
Expressivity	Variable	Variable
Time of onset	Shortly after birth	Before weaning
Frequency of occurrence	Predominantly sporadic	Predominantly sporadic
Associated defects	Urinary and kidney defects	Kidney dysgenesis
Sex bias (M:F)	Short segment (4:1), long segment (1:1)	None (1:1)
Modifier effect	Multigenic and heterogeneous	Dependent on genetic background
Risk to siblings	2.6%–7.6% (short segment), 8.2%–19.1% (long segment)	8.4%–17.1% (before weaning)

enteric neurons may well depend on signals from cells derived from the vagal crest. Thus, a limited variation in the number of vagal crest–derived progenitors that manage to reach the *Gdnf*$^{+/-}$ terminal intestine may trigger an amplified and nonlinear innervation response by sacral crest precursors. This could explain why the number of ganglionic cells is reduced nowhere so much as in the colon of *Gdnf*$^{+/-}$ animals.

Our study shows that loss of a functioning *Gdnf* allele can lead to severe hypoganglionosis and segmental aganglionosis along the GI tracts of affected offspring. Any mutation that reduces the number of neurons that control intestinal motility has the potential of causing dysmotility and its clinical consequences. This is especially true for the large intestine, where, according to our results, the maintenance of a threshold level of muscle innervation seems critical. Severe hypoganglionosis in the terminal intestine may be less tolerable than segmental aganglionosis of more proximal regions of the GI tract. This may explain why a high proportion of the *Gdnf*$^{+/-}$ mice exhibit clinical symptoms involving the colon (84% of the adult mice exhibit varying degrees of colon dilation, and 74% show fecal retention). It is important to note that the diverse intestinal dysmotility presentations are mediated by a single genetic defect. This knowledge may prove to be useful in genetic screening and counseling of families at risk of human HSCR.

There has been a long-standing uncertainty as to whether enteric hypoganglionosis, in addition to the well-recognized aganglionosis of the terminal intestine, may be an essential part of the pathogenesis of HSCR and related disorders (Ehrenpreis 1970). Our mouse data suggest that this is indeed the case. However, a quantitative analysis of neuronal counts along the GI tract of patients with HSCR, on the basis of whole-mount staining techniques, is difficult to achieve. Rather, clinical diagnosis is commonly based on the evaluation of a limited number of randomly selected intestinal sections. This approach is unlikely to properly assess varying degrees of hypoganglionosis, because of the normal fluctuation in neuronal density along the GI tract (Karaosmanoglu et al. 1996; Szabolcs et al. 1996, and the present study). Therefore, verification of general hypoganglionosis, especially if not accompanied by segmental aganglionosis, will remain problematic (Kapur 1999). It follows that general enteric hypoganglionosis and its underlying genetic causes may be much more widespread in the human population than can be estimated by current medical diagnosis. Our results suggest that, in addition to segmental aganglionosis, severe hypoganglionosis is likely an integral mechanism to human HSCR pathogenesis and susceptibility. In particular, our experiments may help to understand the pathogenesis of HSCR in patients who carry mutations in the *c-RET* pathway, because many characteristics of their disease (as reviewed by Pasini et al. [1996]) are so well reflected by our mouse model (table 1).

Despite the paucity of *Gdnf* mutations associated with human HSCR, several features of our animal model, as listed in table 1, draw attention to reduced GDNF function as a possible cause. Phenotypic features of our *Gdnf*$^{+/-}$ mice are dominantly inherited and show an incomplete penetrance, thereby reflecting a main characteristic of prevalent forms of dominant human HSCR. In addition, there are strong parallels with regard to onset and severity of symptoms. Furthermore, a reduced GDNF level has been associated with loss of ganglionic cells in the GI tracts of patients with HSCR (Bär et al. 1997; Martucciello et al. 1998; Ohshiro and Puri 1998). Yet, *Gdnf*$^{+/-}$ mice do not exhibit megacolon, and they lack the sex bias. Both megacolon and sex bias are hallmarks of short-segment human HSCR. Rather, their phenotype resembles the more severe form of long-segment HSCR—possibly because, in both cases, extensive loss of enteric neurons along the GI tract extends proximally into the small intestine. Third, the penetrance of the perinatal mortality in the *Gdnf*$^{+/-}$ mutants is strikingly similar to sibling risk in familial cases of human long-segment HSCR. Regardless of whether the similarity is significant or merely coincidental, it underscores the notion that the obser-

vation of complex phenotypes is compatible with the presence of a defined genetic lesion in a single locus. Obviously, *Gdnf* haploinsufficiency, without concomitant mutations in the coding sequence, is sufficient to cause a spectrum of mild-to-severe phenotypes that are based on varying degrees of hypoganglionosis and segmental aganglionosis. We reason that subthreshold levels of GDNF would result in ganglion loss to a degree incompatible with normal intestinal function and would be followed by clinical symptoms of HSCR.

On the basis of a population study of 2,000 $Gdnf^{+/-}$ mice in three genetic backgrounds, we find that as many as 90% of these mutant animals are in a susceptible state. They are more likely than are wild-type mice to produce offspring that develop HSCR, with a low but significant incidence of postnatal death in the various $Gdnf^{+/-}$ cohorts. This allowed us to assess susceptibility to a complex disease, a fundamental issue that is not easily amenable to genetic evaluation in humans. Taken together, our results suggest that the *Gdnf* locus may be more frequently associated with human HSCR than has hitherto been realized, whether through mutations in the GDNF gene itself or in any other gene that affects GDNF signaling efficacy. Our findings offer a plausible way to connect an array of seemingly disparate features that are characteristic of a complex disease to a much more narrowly defined genetic cause. The lessons we learned in linking a low penetrance of symptoms to disease susceptibility demonstrate that a broad-based population study in genetically defined mutant strains can be an effective alternative approach to the dissection of the genetic basis of complex human disorders (Bedell et al. 1997*a,* 1997*b;* Justice 2000).

Acknowledgments

We would like to express our appreciation to Dr. Raj P. Kapur for providing us with the *DβH-nLacZ* transgenic mice. We also thank Drs. Stuart Yuspa, Raj P. Kapur, and Karl Pfeifer for their critical reading of the manuscript and for insightful comments. L.S. received a Research Associateship from National Research Council.

Electronic-Database Information

Accession numbers and the URL for data in this article are as follows:

Online Mendelian Inheritance in Man (OMIM), http://www.ncbi.nlm.nih.gov/Omim/ (for HSCR [mim 142623]; WS4 [MIM 277580]; EDN3 [MIM 131242]); EDNRB [MIM 121244)]; and c-RET [MIM 164761]).

References

Angrist M, Bolk S, Halushka M, Lapchak PA, Chakravarti A (1996) Germline mutations in glial cell line-derived neurotrophic factor (*GDNF*) and *RET* in a Hirschsprung disease patient. Nat Genet 14:341–344

Angrist M, Bolk S, Thiel B, Puffenberger EG, Hofstra RM, Buys CHCM, Cass DT, Chakravarti A (1995) Mutation analysis of the RET receptor tyrosine kinase in Hirschsprung disease. Hum Mol Genet 4:821–830

Attié T, Pelet A, Edery P, Eng C, Mulligan LM, Amiel J, Boutrand L, Beldjord C, Nihoul-Fékété C, Munnich A, Ponder BAJ, Lyonnet S (1995) Diversity of *RET* proto-oncogene mutations in familial and sporadic Hirschsprung disease. Hum Mol Genet 4:1381–1386

Badner JA, Sieber WK, Garver KL, Chakravarti A (1990) A genetic study of Hirschsprung disease. Am J Hum Genet 46: 568–580

Bär KJ, Facer P, Williams NS, Tam PK, Anand P (1997) Glial-derived neurotrophic factor in human adult and fetal intestine and in Hirschsprung's disease. Gastroenterology 112: 1381–1385

Baynash AG, Hosoda K, Giaid A, Richardson JA, Emoto N, Hammer RE, Yanagisawa M (1994) Interaction of endothelin-3 with endothelin-B receptor is essential for development of epidermal melanocytes and enteric neurons. Cell 79:1277–1285

Bedell MA, Jenkins NA, Copeland NG (1997*a*) Mouse models of human disease. I. Techniques and resources for genetic analysis in mice. Genes Dev 11:1–10

Bedell MA, Largaespada DA, Jenkins NA, Copeland NG (1997*b*) Mouse models of human disease. II. Recent progress and future directions. Genes Dev 11:11–43

Berry CL, Keeling JW (1996) Gastrointestinal system. In: Berry CL (ed) Paediatric pathology. Springer, New York, pp 207–275

Burns AJ, Le Douarin NM (1998) The sacral neural crest contributes neurons and glia to the post-umbilical gut: spatiotemporal analysis of the development of the enteric nervous system. Development 125:4335–4347

Cacalano G, Farinas I, Wang LC, Hagler K, Forgie A, Moore M, Armanini M, Phillips H, Ryan AM, Reichardt LF, Hynes M, Davies A, Rosenthal A (1998) GFRα1 is an essential receptor component for GDNF in the developing nervous system and kidney. Neuron 21:53–62

Chakravarti A (1996) Endothelin receptor-mediated signaling in Hirschsprung's disease. Hum Mol Genet 5:303–330

Durbec PL, Larsson-Blomberg LB, Schuchardt A, Costantini F, Pachnis V (1996) Common origin and developmental dependence on c-ret of subsets of enteric and sympathetic neuroblasts. Development 122:349–358

Edery P, Attié T, Amiel J, Pelet A, Eng C, Hofstra RMW, Martelli H, Bidaud C, Munnich A, Lyonnet S (1996) Mutation of the endothelin-3 gene in the Waardenburg-Hirschsprung disease (Shah-Waardenburg syndrome). Nat Genet 12:442–444

Edery P, Lyonnet S, Mulligan L, Pelet A, Dow E, Abel L, Holder S, Nihoul-Fékété C, Ponder B, Munnich A (1994) Mutations of the *RET* proto-oncogene in Hirschsprung's disease. Nature 367:378–380

Ehrenpreis T (1970) Hirschsprung diseases. Year Book Medical Publishers, Chicago

Enomoto H, Araki T, Jackman A, Heuckeroth RO, Snider WD, Johnson EMJ, Milbrandt J (1998) GFRα1-deficient mice have deficits in the enteric nervous system and kidneys. Neuron 21:317–324

Gershon MD (1995) Neural crest development: do developing enteric neurons need endothelins? Curr Biol 5:601–604

Gershon MD, Kirchgessner AL, Wade PR (1994) Functional anatomy of the enteric nervous system. In: Johnson LR (ed) Physiology of the gastrointestinal tract. Raven Press, New York, pp 381–422

Holschneider AM (1982) Hirschsprung's disease. In: Holschneider AM (ed). Hippokrates Verlag, Stuttgart

Holschneider AM, Meier-Ruge W, Ure BM (1994) Hirschsprung's disease and allied disorders: a review. Eur J Pediatr Surg 4:260–266

Hosoda K, Hammer RE, Richardson JA, Baynash AG, Cheung JC, Giaid A, Yanagisawa M (1994) Targeted and natural (piebald-lethal) mutations of endothelin-B receptor gene produce megacolon associated with spotted coat color in mice. Cell 79:1267–1276

Ivanchuk SM, Myers SM, Eng C, Mulligan LM (1996) De novo mutation of GDNF, ligand for the RET/GDNFR-a receptor complex, in Hirschsprung disease. Hum Mol Genet 5:2023–2026

Justice M (2000) Capitalizing on large-scale mouse mutagenesis screens. Nat Rev Genet 1:109–115

Kapur RP (1999) Hirschsprung disease and other enteric dysganglionoses. Crit Rev Clin Lab Sci 36:225–273

Kapur RP, Hoyle GW, Mercer EH, Brinster RL, Palmiter RD (1991) Some neuronal cell populations express human dopamine β-hydroxylase-*lacZ* transgenes transiently during embryonic development. Neuron 7:717–727

Karaosmanoglu T, Aygun B, Wade PR, Gershon MD (1996) Regional differences in the number of neurons in the myenteric plexus of the guinea pig small intestine and colon: an evaluation of markers used to count neurons. Anat Rec 244: 470–480

Kusafuka T, Puri P (1997) Mutations of the endothelin-B receptor and endothelin-3 genes in Hirschsprung's disease. Pediatr Surg Int 12:19–23

Martucciello G, Thompson H, Mazzola C, Morando A, Bertagnon M, Negri F, Brizzolara A, Rocchetti L, Gambini C, Jasonni V (1998) GDNF deficit in Hirschsprung's disease. J Pediatr Surg 33:99–102

Mercer EH, Hoyle GW, Kapur RP, Brinster RL, Palmiter RD (1991) The dopamine b-hydroxylase gene promoter directs expression of *E. coli lacZ* to sympathetic and other neurons in adult transgenic mice. Neuron 7:703–716

Milla PJ (1996) Intestinal motility during ontogeny and intestinal pseudo-obstruction in children. Pediatr Clin North Am 43:511–532

Moore MW, Klein RD, Fariñas I, Sauer H, Armanini M, Phillips H, Reichardt LF, Ryan AM, Carver-Moore K, Rosenthal A (1996) Renal and neuronal abnormalities in mice lacking GDNF. Nature 382:76–79

Ohshiro K, Puri P (1998) Reduced glial cell line-derived neurotrophic factor level in aganglionic bowel in Hirschsprung's disease. J Pediatr Surg 33:904–908

Pasini B, Ceccherini I, Romeo G (1996) RET mutations in human disease Trends Genet 12:138–144

Pichel JG, Shen L, Sheng HZ, Granholm AC, Drago J, Grinberg A, Lee EJ, Huang SP, Saarma M, Hoffer BJ, Sariola H, Westphal H (1996) Defects in enteric innervation and kidney development in mice lacking GDNF. Nature 382:73–76

Pomeranz HD, Gershon MD (1990) Colonization of avian hindgut by cells derived from the sacral neural crest. Dev Biol 137:378–394

Pomeranz HD, Rothman TP, Gershon MD (1991) Colonization of the post-umbilical bowel by cells derived from the sacral neural crest: direct tracing of cell migration using an intercalating probe and a replication-deficient retrovirus. Development 111:647–655

Puffenberger EG, Hosoda K, Washington SS, Nakao K, deWit D, Yanagisawa M, Chakravarti A (1994) A missense mutation of the endothelin-B receptor gene in multigenic Hirschsprung's disease. Cell 79:1257–1266

Puri P, Ohshiro K, Wester T (1998) Hirschsprung's disease: a search for etiology. Semin Pediatr Surg 7:140–147

Qualman SJ, Murray R (1994) Aganglionosis and related disorders. Hum Pathol 25:1141–1149

Romeo G, Ronchetto P, Luo Y, Barone V, Seri M, Ceccherini I, Pasini B, Bocciardi R, Lerone M, Kaariainen H, Martucciello G (1994) Point mutations affecting the tyrosine kinase domain of the *RET* proto-oncogene in Hirschsprung's disease. Nature 367:377–378

Salomon R, Attié T, Pelet A, Bidaud C, Eng C, Amiel J, Sarnacki S, Goulet O, Ricour C, Nihoul-Fékété C, Munnich A, Lyonnet S (1996) Germline mutations of the RET ligand GDNF are not sufficient to cause Hirschsprung disease. Nat Genet 14:345–347

Sánchez MP, Silos-Santiago I, Frisén J, He B, Lira SA, Barbacid M (1996) Renal agenesis and the absence of enteric neurons in mice lacking GDNF. Nature 382:70–73

Schuchardt A, D'Agati V, Larsson-Blomberg L, Costantini F, Pachnis V (1994) Defects in the kidney and enteric nervous system of mice lacking the tyrosine kinase receptor Ret. Nature 367:380–383

Serbedzija GN, Burgan S, Fraser SE, Bronner-Fraser M (1991) Vital dye labeling demonstrates a sacral neural crest contribution to the enteric nervous system of chick and mouse embryos. Development 111:857–866

Szabolcs MJ, Visser J, Shelanski ML, O'Toole K, Schullinger JN (1996) Peripherin: a novel marker for the immunohistochemical study of malformations of the enteric nervous system. Pediatr Pathol Lab Med 16:51–70

Weinberg AG (1975) Hirschsprung's disease: a pathologist's view. Perspect Pediatr Pathol 2:207–239

Yin L, Barone V, Seri M, Bolino A, Bocciardi R, Ceccherini I, Pasini B, Tocco T, Lerone M, Cywes S, Moore S, Vanderwinden JM, Abramowicz MJ, Kristofferson U, Larsson LT, Hampel BJC, Silengo M, Martucciello G, Romeo G (1994) Heterogeneity and low detection rate of RET mutations in Hirschsprung disease. Eur J Hum Genet 2:272–280